Article ID: 1003－6326(2003)04－0998－05

Preparation and electrochemical properties of nanosized tin dioxide electrode material by sol-gel process①

HE Ze-qiang(何则强)[1], LI Xin-hai(李新海)[1], WU Xian-ming(吴显明)[2],
HOU Zhao-hui(侯朝辉)[1], LIU En-hui(刘恩辉)[1], DENG Ling-feng(邓凌峰)[1],
HU Chuan-yue(胡传跃)[1], TIAN Hui-peng(田慧鹏)[1]
(1. School of Metallurgical Science and Engineering,
Central South University, Changsha 410083, China;
2. College of Chermistry and Chemical Engineering, Jishou University, Jishou 416000, China)

Abstract: Nanosized SnO_2 powders were prepared by sol-gel process using inorganic salt as a precursor. The tin oxide powders obtained at different calcinating temperatures (300－700 ℃) were investigated by means of X-ray diffraction (XRD), infrared spectrum (IR), thermogravimetric analysis (TGA), differential thermal analysis (DTA) and transmission electron microscopy (TEM) as well. The results indicate that well-crystallized nanosized SnO_2 powders with a structure of rutile and uniform size about 10 nm can be obtained when the calcinating is carried out at 550 ℃ for 3 h using the method. The electrochemical properties of nanosized SnO_2 powders as anode material for lithium ion batteries were also studied in detail. The results show that nanosized SnO_2 is a candidate of anode material for lithium ion batteries with reversible capacity more than 372 mA·h/g after ten cycles and low voltage for Li^+ intercalation and de-intercalation.

Key words: tin dioxide; nanosized materials; sol-gel method; lithium ion batteries; anode; electrochemical properties
CLC number: O 481.4; TM 912.9 **Document code:** A

1 INTRODUCTION

Tin oxide is a wide energy gap semiconductor and has found many technological applications such as catalysts for oxidation of organics, solid-state gas sensors and optical electronic devices[1,2]. Recently, several tin-oxide-based compounds were reported to be good candidates as anodes for lithium ion batteries instead of carbonaceous electrodes[3－6], the electrochemical reaction occurring in these compounds is not the intercalation of lithium into a host structure. For bulk samples of amorphous and crystalline tin oxide, a decomposition reaction initially leads to the formation of metallic tin in Li_2O matrix, followed by the formation of Li-Sn alloy, thus leading to a high reversible capacity of 800 mA·h/g at a low potential vs lithium. Furthermore, these tin oxides are stable in air and standard electrolytes. Many researchers[4－8] pointed out that only nanocrystallites of tin oxide materials are efficient for such negative electrodes and an increase in particle size drastically decreases their reversible capacity.

The capacity of electrode material is critically affected by the morphology of the material which contributes to different ways of the diffusion processes of Li^+. Nanostructure electrode material is not only a good model system for the research of intercalation reaction of Li^+, but also a promising material in some special lithium ion battery systems such as micro-batteries[7－9]. In this paper, nanosized tin oxide were prepared by sol-gel process using inorganic salt as a precursor. The microstructure and electrochemical properties of nanosized SnO_2 as anode material for lithium ion batteries were investigated in detail.

2 EXPERIMENTAL

2.1 Preparation process

Aqueous solution of $SnCl_4$ was made by dissolving analytically pure $SnCl_4 \cdot 5H_2O$ in distilled water while hydrochloric acid was added into the solution to avoid formation of $SnO(OH)_2$. The solution was then continuously stirred with addition of aqueous ammonia and additives until formation of desired sol. The sol was kept at a suitable temperature for a while, then gel was obtained. The gel was repeatedly washed with distilled water to remove Cl^-, then dispersed by ultrasonic vibration and dried in vacuum at 80 ℃ for 2 d. The granules were ground to obtain white powders of dry gel, the samples were obtained after calcinating the dry gel powders at 300－700 ℃

① **Received date:** 2002－08－04; **Accepted date:** 2002－11－22
Correspondence: HE Ze-qiang, PhD; Tel: +86-731-8832487; Fax: +86-731-8836633; E-mail: csuhzq@163.com

for 3 h.

2.2 Characterization of material

Thermal behavior of the dry gel was investigated by TGA and DTA on a TGA-SDTA851^e thermal analysis system (Mettler Toledo Corp.) from 25 ℃ to 800 ℃ in Ar atmosphere at a heating rate of 10 ℃/min; infrared spectra measurement was conducted in a Fourier-transform infrared spectrometer (Nicolet Corp.); phase identification were carried out by XRD (Rigaku D/MAX-gA). In order to determine the size of SnO_2 crystallites, instrumental broadening was estimated with a standard silicon sample and taken into account in the grain size estimation using Scherrer's formula. The microstructure of the powders were characterized by TEM (JEOL 2000X).

2.3 Electrochemical tests

A slurry containing (mass fraction) 80% synthesized material, 10% acetylene black and 10% PVDF (polyvinylidene fluoride) was made using NMP (N-methylprrolidinone) as the solvent. Electrodes with an area of 1 cm^2 for the measurements of electrochemical characterization were prepared by coating the slurries (about 100 μm in thickness) on copper foils, followed by drying in vacuum at 120 ℃ for 12 h. The mass of active material on the electrodes was 2.0 – 6.0 mg/cm^2. All electrode compositions referred to mass fraction and the capacity of the electrodes were calculated on the basis of the mass of active materials (excluding binder and conducting agent).

Electrochemical tests were conducted using a conventional coin-type cell, lithium foil as a counter electrode and 1.0 mol/L $LiPF_6$ in ethylene carbonate /dimethyl carbonate (EC/DMC) (φ(EC)/φ(DMC) = 1) as the electrolyte. The assembly was carried out in an Ar-filled glove box. The discharge-charge tests were done under a constant current density of 0.20 mA/cm^2 in a voltage window of 0 – 2.0 V or 0 – 1.0 V. Discharging and charging of the cell refer to insertion and extraction of lithium into/from SnO_2 electrode respectively. The rest time between the discharge and charge is 30 min, the voltage used here is vs Li/Li^+. All the electrochemical analyses were carried out with an electrochemical analysis system.

3 RESULTS AND DISCUSSION

3.1 Thermal analysis

Fig. 1 shows TG curve and DTA curve of the dry gel. The mass loss of dry gel consists of three parts: the first mass loss takes place at 25 – 120 ℃ on TG curve, accordingly, there is a strong endothermic peak on DTA curve at 95 ℃, which is due to the evaporation of physical absorbed water on the surface of the dry gel[10]; the second mass loss is found at 120 – 350 ℃ on TG curve and there is a wide exothermic peak at 120 – 350 ℃ on DTA curve, which is assigned to the decomposition of small amount of ammonium chloride and organic compound[11]; the third mass loss is not very clear on TG curve at 350 – 510 ℃, but a big exothermic peak can be seen on DTA curve, which is caused by the ordering of the irregularly distributed atoms and the integrity of crystals. Over 510 ℃, no mass loss takes place on TG curve, which indicates the crystallization tends to complete at about 510 ℃.

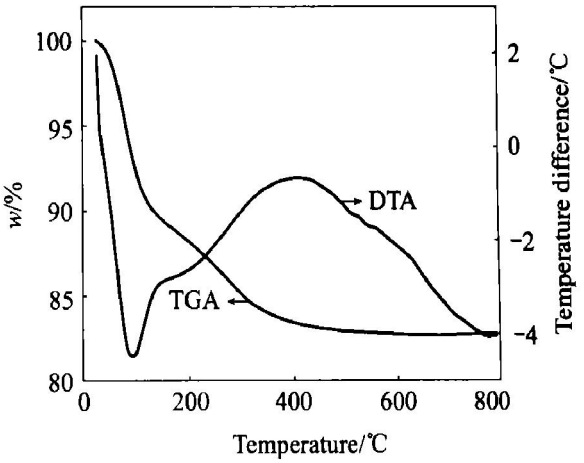

Fig. 1 TGA—DTA curves of dry gel

3.2 IR spectrum of dry gel

IR spectrum of the dry gel is shown in Fig. 2. The striking bands at 571 cm^{-1} and 1 086 cm^{-1} correspond to the Sn-O stretching and vibration from Sn-OH[12]. The bands corresponding to deformation of both – OH of physically adsorbed water and – NH of ammonia appear in the range of 1 400 cm^{-1} to 1 600 cm^{-1}[11]. The band at 3 422 cm^{-1} is assigned to the stretching vibration of – OH which is absorbed on the surface of SnO_2 by a great deal of dangling bonds[12].

3.3 X-ray diffraction

Fig. 3 shows the XRD patterns of dry gel and

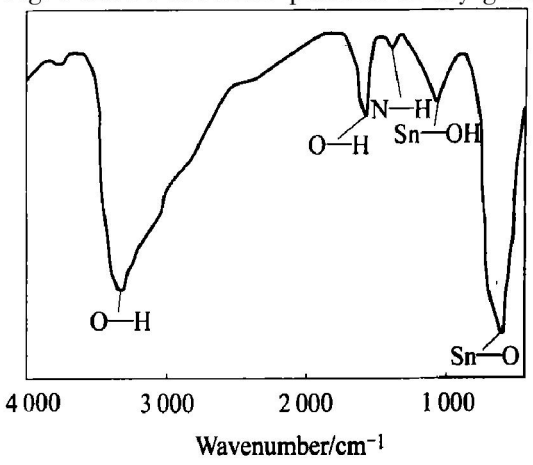

Fig. 2 IR spectrum of dry gel

the samples treated at different temperatures. There are only wide and weak diffraction peaks on the XRD patterns of dry gel and sample calcinated at 300 ℃, which indicates that they are amorphous. Well-crystallized nanosized SnO_2 powders were obtained above 550 ℃ for consecutive dehydration of —OH group, which agrees well with the results derived from the thermal analysis. The strong diffraction peaks of the samples marked with (110), (101) and (211) are identical with the pattern of tetragonal SnO_2 with rutile structure (JCPDS file number 21-1250). With increasing calcinating temperature, these diffraction peaks are sharpened and enhanced, which shows the particles have grown up with more perfect crystalline. The physical characteristics of crystallites change with the average size of crystallite decreasing, resulting in the peaks widening in the XRD patterns.

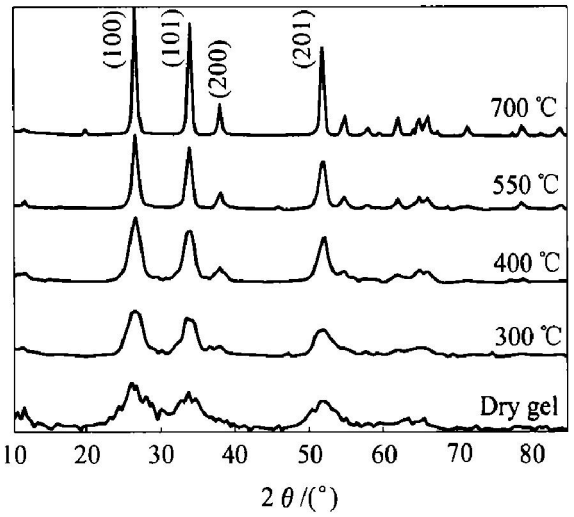

Fig. 3 XRD patterns of dry gel and powders calcinated at different temperatures for 3 h

The average size of particles calcinated at 300 ℃ to 700 ℃ is 9 ~ 12 nm, based on lattice parameters of the (110) plane by Scherrer formula:

$$D = k\lambda / \beta\cos\theta$$

where D is the crystallite size, k is the Scherrer constant ($k = 0.9$, assuming that the particles are spherical), λ is the wavelength of the X-ray radiation (CuK_α radiation, $\lambda = 0.154$ nm), β is the half-maximum line breadth and θ is the diffraction angle.

The plot of size of SnO_2 powders vs calcinating temperature is shown in Fig. 4. With increasing calcinating temperature, the average size of nanosized SnO_2 powders increases. The kinetics of grain growth is controlled by grain boundary diffusion in lower temperature regions, and by the evaporation-condensation mechanism in higher temperature regions[13]. When the calcinating temperature is below 400 ℃, the average size of the powders increases slowly with increasing temperature. However, the grain size increase rapidly

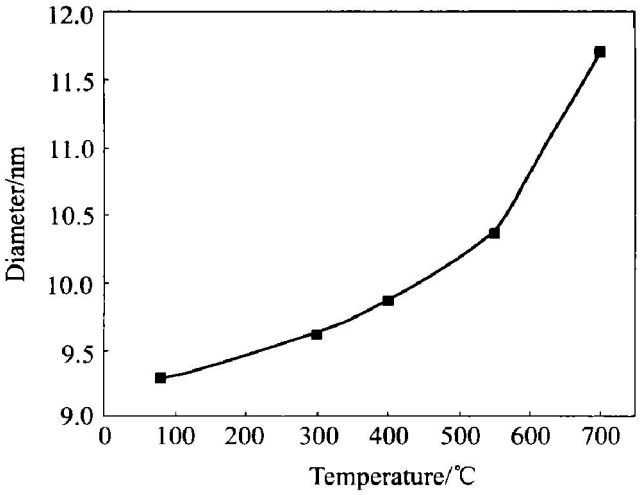

Fig. 4 Plot of size of SnO_2 powders vs calcinating temperature

when the calcinating temperature is 550 ℃ and above 550 ℃.

3.4 TEM micrograph

TEM micrograph of the SnO_2 powders calcinated at 550 ℃ for 3 h in air is presented in Fig. 5. The average size of the sample is about 10 nm, which agrees well with the value calculated by Scherrer formula. The fine particles are spherical and each particle is an aggregation of a few small crystallites.

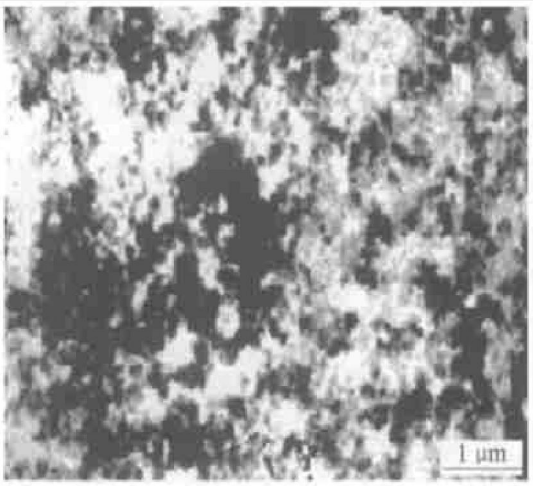

Fig. 5 TEM micrograph of nanosized SnO_2 powders calcinated at 550 ℃

3.5 Electrochemical characteristics

The first discharge-charge curve of nanosized SnO_2 electrode material is shown in Fig. 6. The two pseudo plateau in the discharge curve can be interpreted in initial formation of Sn, followed by formation of an Li_xSn alloy. The first discharge capacity from rest potential to naught at a constant current density of 0.2 mA/cm^2 reaches about 1 660 mA·h/g. The charge capacity from 0 to 2.0 V at a constant current density of 0.2 mA/cm^2 also shows a high value over 687 mA·h/g. Thus, the irreversible capacity for the first cycle is about

973 mA·h/g, corresponding to an irreversible loss of about 59%, which is slightly larger than the predicted theoretical value of 48%. The values of Li/Sn for discharge and charge are about 7.35 and 3.04, respectively. The result suggests that the nanosized SnO_2 can be used as an anode for lithium secondary batteries with high capacity, however the first cycle of nanosized SnO_2 electrode exhibits enormous irreversible capacity, which is mainly attributed to the electrolyte decomposition and the film formation on the large surface of nanosized SnO_2 powders and the reduction of tin oxide[14-16].

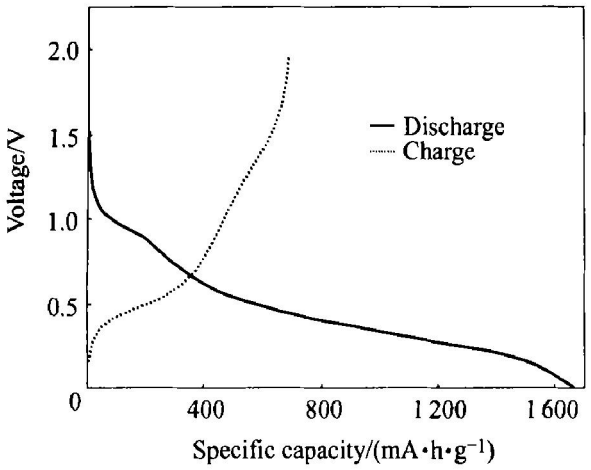

Fig. 6 First discharge and charge curve of nanosized SnO_2 anode

Differential capacity (dQ/mdV)-voltage plots for the first, the second and the tenth cycle are shown in Fig. 7. The solid line represents the first discharge and charge curve and the rest lines are the subsequent charge and discharge curves. The first discharge profiles are substantially similar to those observed for bulk SnO_2 and SnO_2 film[17-19]. There is a sharp peak in the range of 0.9 - 1.0 V, which corresponds to the reaction between tin oxide and lithium leading to the dissociation of oxide. The differential peaks appearing between 0.2 V and 0.5 V during discharge and charge are very reproducible, which are associated with the alloying reactions between Sn and Li. These peaks may represent different states of lithium stored in the form of Li_xSn alloys[5]. The reaction of lithium and Sn to form Li_xSn alloys can result in a volume increase of 300%, which can induce serious cracking or crumbling of Li_xSn alloy[6]. Cracking of the Li-Sn alloys will cause isolation of Sn, increase impedance and eventually decrease capacity of the electrode. This is why the capacity of the electrode of nanosized SnO_2 in the tenth cycle becomes much lower than that in the first cycle.

Cyclability of nanosized SnO_2 electrode at different voltage windows is presented in Fig. 8 and Fig. 9. Obviously, the range of the voltage for cycling tes-

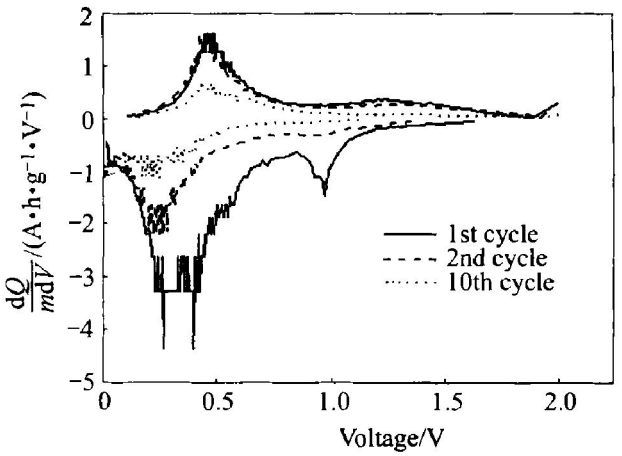

Fig. 7 Differential capacity-voltage plots of nanosized SnO_2 electrode during cycling

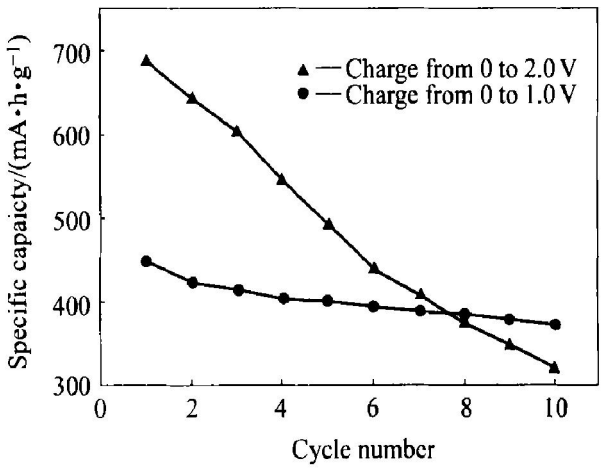

Fig. 8 Relationship between specific capacity and cycle number for different voltage windows

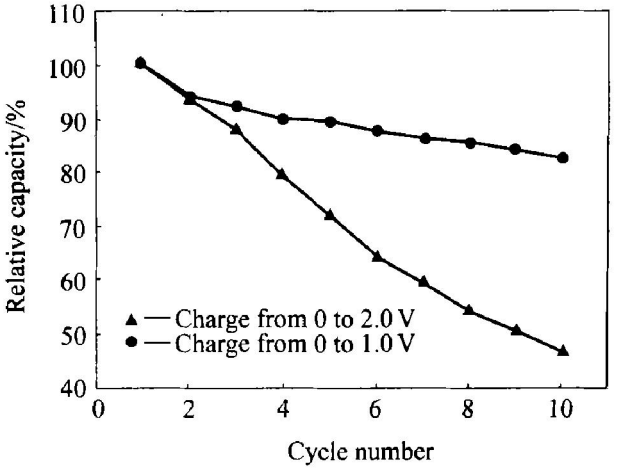

Fig. 9 Relative capacity of different cycle in different voltage windows

ts has great influence on the cycling performance. The capacity retention (the relative capacity of different cycles to the first cycle) of SnO_2 electrode was greatly improved when the upper cutoff voltage change 2.0 V for 1.0 V. This may be due to the increase of volume change in the formation of low con-

tent of Li in the Li-Sn alloy, which results in cracking and crumbling of the electrode those crystals. Ref. [4] thought, the discharge-charge from 0 to 1.0 V prevents destroying Li_2O matrix which holds the Sn atoms on the electrode. The range of 0 to 1.0 V is found to be better voltage window with a view of minimizing capacity loss while maintaining high specific capacity in the first charging process. Because different voltage windows can influence the size of the tin regions and apparently cause aggregation of tin as a function of the number of cycles, thus leading to capacity fade in the cell[20]. Therefore examining the cycling behavior of anode requires selecting the most suitable working voltage limits.

4 CONCLUSIONS

Nanosized tin dioxide with structure of rutile can be prepared by sol-gel process using inexpensive inorganic salt $SnCl_4$ as a precursor and a little additive as sol forming auxiliary. The sample calcinated at 550 ℃ has an average grain size of about 10 nm. Nanosized SnO_2 electrode delivers large capacity of initial lithium insertion and extraction with 1 660 mA·h/g and 687 mA·h/g respectively. However, the capacity degrade quickly with increasing cycling number, especially when a voltage window of 0 - 2.0 V was used to discharge and charge. This problem may be solved by producing SnO_2 powders with appropriate crystal structure and microstructure and selecting suitable cutoff voltage for charge and discharge. Consequently, there may be potential applications for nanosized tin dioxide as anode material with high specific capacity in lithium ion batteries.

REFERENCES

[1] Qi L M, Ma J M, Cheng H M, et al. Synthesis and characterization of mesostructured tin oxide with crystalline walls [J]. Langumuir, 1998, 14: 2579 - 2581.

[2] Göpel W, Schierbaum K D. SnO_2 sensors: current status and future prospects [J]. Sensors and Actuators B, 1995, 26/27: 1 - 12.

[3] Idota Y, Kubota T, Matsufuji A, et al. Tin-based amorphous oxide: A high-capacity lithium ion storage material [J]. Science, 1997, 276: 1395 - 1397.

[4] Courtney I A, Dahn J R. Key factors controlling the reversibility of the reaction of lithium with SnO_2 and Sn_2BPO_6 glass [J]. J Electrochem Soc, 1997, 144(9): 2943 - 2948.

[5] Courtney I A, Dahn J R. Electrochemical and in situ X-ray diffraction studies of the reaction of lithium with tin oxide composites [J]. J Electrochem Soc, 1997, 144(6): 2045 - 2052.

[6] Liu W F, Huang X J, Wang Z X, et al. Studies of stannic oxide as an anode material for lithium - ion batteries [J]. J Electrochem Soc, 1998, 145(1): 59 - 62.

[7] Li N C, Charles R M, Bruno S. Nanomaterial-based Li-ion battery electrodes [J]. Journal of Power Sources, 2001(97/98): 240 - 243.

[8] Whitehead A H, Elliott J M, Owen J R. Nanostructure tin for use as a negative electrode material in Li-ion batteries [J]. Journal of Power Sources, 1999(81/82): 33 - 38.

[9] Mao O, Turner R L, Courtney I A, et al. Active/inactive nanocomposites as anodes for Li-ion batteries [J]. Electrochemical and Solid-State Letters, 1999, 2(1): 3 - 5.

[10] Shiomi H, Akakimoto C, Nakahir A A, et al. Preparation of SnO_2 monolithic gel by sol-gel method [J]. Journal of Sol-Gel Science and Technology, 2000, 19: 759 - 763.

[11] Kobayashi Y, Okamoto M, Tomita A. Preparation of tin oxide monolith by the sol-gel method from inorganic salt [J]. J Mater Sci, 1996, 31: 3125 - 6127.

[12] Hiratsuka R S, Pulcinelli S H, Santilli C V. Formation of SnO_2 gels from dispersed sol in aqueous colloidal solutions [J]. J Non-cryst Solids, 1990, 121: 76 - 83.

[13] Kimura T, Inada S, Yamaguchi T. Microstructure development in SnO_2 with and without additives [J]. J Mater Sci, 1989, 24: 220 - 226.

[14] Kim J Y, King D E, Kumta P N, et al. Chemical synthesis of tin oxide-based materials for Li-ion battery anodes: Influence of process parameters on the electrochemical behavior [J]. J Electrochem Soc, 2000, 147(12): 4411 - 4420.

[15] Li H, Shi L H, Liu W, et al. Studies on capacity loss and capacity fading of nanosized SnSb alloy anode for Li-ion batteries [J]. J Electrochem Soc, 2001, 148(8): A915 - 922.

[16] Yang J, Takeda Y, Imanishi N, et al. Tin-containing anode materials in combination with $Li_{2.6}Co_{0.4}N$ for irreversibility compensation [J]. J Electrochem Soc, 2000, 147(5): 1671 - 1676.

[17] Mohamedi M, Lee S J, Takahashi D, et al. Amorphous tin oxide films: preparation and characterization as an anode active material for lithium ion batteries [J]. Electrochemical Acta, 2001, 46: 1161 - 1168.

[18] Yu A, Roger F. Mesoporous tin oxides as lithium intercalation anode materials [J]. Journal of Power Sources, 2002, 104: 97 - 100.

[19] Machill S, Shodai T, Sakurai Y, et al. Electrochemical characterization of tin based composite oxides as negative electrodes for lithium batteries [J]. Journal of Power Sources, 1998, 73(2): 216 - 223.

[20] Morales J, Sanchez L. Electrochemical behaviour of SnO_2 doped with boron and indium in anodes for lithium secondary batteries [J]. Solid State Ionics, 1999, 126: 219 - 226.

(Edited by YANG Hua)